Materials Processing Fundamentals
Edited by: Princewill Anyalebechi
TMS (The Minerals, Metals & Materials Society), 2007

INFLUENCE OF PROCESS PARAMETERS ON THE PHASE TRANSFORMATION AND CONSEQUENT HARDNESS INDUCED BY THE LENS™ PROCESS

Liang Wang[1] and Sergio Felicelli[2]

[1]Center for Advanced Vehicular Systems, Mississippi State University, Mississippi State, MS 39762; email: liangw@cavs.msstate.edu
[2]Mechanical Engineering Department, Mississippi State University, Mississippi State, MS 39762; email: felicelli@me.msstate.edu

Keywords: Laser Engineered Net Shaping, LENS, phase transformation, hardness

Abstract

A three-dimensional finite element model was developed to predict the temperature distribution and phase transformation in deposited stainless steel 410 (SS410) during the Laser Engineered Net Shaping (LENS™) rapid fabrication process. The development of the model was carried out using the SYSWELD software package. The model calculates the evolution of temperature in the part during the fabrication of a SS410 plate. The metallurgical transformations are taken into account using the temperature dependent material properties and the continuous cooling transformation diagram. The ferritic and martensitic transformation, as well as austenitization and tempering of martensite are considered. The influence of processing parameters such as laser power and traverse speed on the phase transformation and the consequent hardness are analyzed. The potential presence of porosity due to lack of fusion is also discussed. The results show that the temperature distribution, the microstructure and properties in the final part depend significantly on the processing parameters.

Introduction

The Laser Engineering Net Shaping (LENS™) process is a laser-assisted, direct metal manufacturing process for rapid fabrication [1-3]. Figure 1 shows the schematic of the LENS fabrication process. The LENS fabricated part is built on a solid substrate usually made of the metal to be deposited or similar material. Initially, the laser beam is focused on the substrate to create a molten pool, where metallic powder particles are simultaneously injected by a set of converging nozzles. A single layer of material is built up when the substrate moves beneath the laser beam in the x-y plane under computer guidance. After deposition of a single layer, the laser beam and the powder delivery nozzle assembly is incremented in the positive z-direction to begin the deposition of subsequent layers. Accordingly, the process is repeated and a three-dimensional part is built up in a layer-by-layer manner.

The feasibility of depositing different metals including stainless steel, tool steel, nickel-based superalloys and titanium into near-net shape parts in a single processing step has been illustrated

using LENS rapid fabrication technology in the past [4-6]. However, the non-uniform microstructure and properties found in the parts built by LENS may restrain the wide acceptance of this process in industry [6]. In order to fully understand the microstructure and properties of LENS-deposited materials, it is essential to investigate the effects of processing parameters on the thermal history at each point of the part, as well as the solid-state phase transformations that may occur during the process. Numerical simulation methods have the potential to provide such knowledge based on a suitable physical computational model. Numerical models have been undertaken by several authors to simulate the thermal behavior [1-8] and microstructure evolution [9-15] during the laser deposition process. The results of these models can provide insight into how processing parameters can be manipulated to obtain favorable metallurgical structures and mechanical properties.

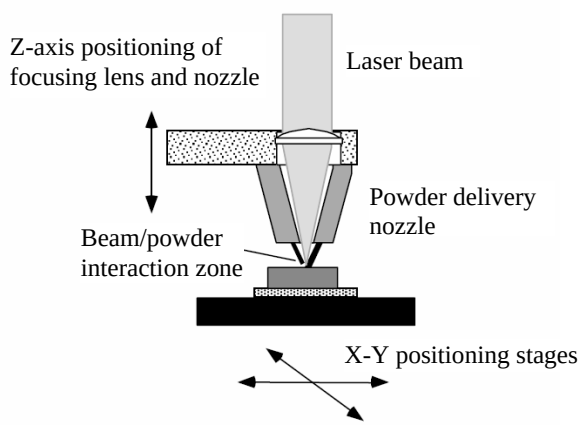

Figure 1. Schematic of the LENS process.

When a layer of material is being deposited, several previously deposited layers can be reheated or remelted, which under unfavorable process conditions may lead to undesired effects. For example, during the LENS deposition of steel, martensite can be reheated above the martensite start temperature, leading to tempered martensite after posterior cool-down. However, if the process parameters are controlled such that most of the part remains at temperatures higher than the martensite start temperature, after cool-down this will lead to a uniform microstructure consisting of non-tempered martensite with minor proportions of retained austenite and carbides. The resulting hardness is also high and uniformly distributed [9-11]. Costa et al. [12-14] investigated the effects of the substrate size and the idle time between the deposition of consecutive layers of material on the phase transformation and hardness distribution in SS420 parts built by a laser powder deposition process similar to LENS. They found that short idle time and small substrate size can reduce the proportion of tempered martensite and lead to a more uniform microstructure and property distribution. This is because both short idle time and small substrate size are more probable to keep most of the part at temperatures higher than the martensite start temperature.

The size of the molten pool is a suitable monitor to optimize the processing parameters during the LENS process. The temperature distribution and cooling rate at the solid-liquid interface of the molten pool affect the microstructural features, which determine the strength and ductility of the deposited part. Therefore, control of the molten pool determines the properties of the resulting solidified product [5]. The effects of the laser-processing parameters (laser power and scanning speed) on the molten pool size have been investigated both by experiments [16] and modeling [17-18].

In this model, a heat transfer calculation is coupled with solid phase transformation kinetics data on the ferritic and martensitic transformation and austenitization using the SYSWELD software package [19-21]. By calculating the phase transformations in a SS410 plate during the LENS deposition, the model can infer consequent changes in the hardness of the deposited part. The laser power is adjusted and optimized in order to produce a pre-defined steady molten pool size for different laser traverse speeds. The effects of laser power and traverse speed on the thermal history, phase proportions, and consequent hardness of the processed material during the LENS deposition of a ten-layer wall of SS410 are studied. The potential presence of porosity due to the lack of fusion in certain regions of the part is also discussed.

Mathematical Model

A three-dimensional finite element model was developed to simulate the LENS process using the commercial code SYSWELD. The model was used to predict the temperature distribution and solid-phase transformation of a thin-walled structure (plate) of AISI 410 stainless steel (SS410).

Heat Transfer Analysis

In the heat transfer calculations, the heat conduction equation was solved numerically using the finite element method. The density, thermal conductivity, and specific heat are dependent on temperature and material phase. In addition to the solid phase transformations, the latent heat of the solid-liquid phase change is also considered through the enthalpy function. It was assumed that the substrate material is initially at room temperature, T_0 (no pre-heating). A fixed temperature boundary condition equal to the room temperature is prescribed on the bottom surface of the substrate. The boundary conditions for all other surfaces take into account both laser heating and heat losses due to surface convection and radiation. The laser beam power is modeled as a Gaussian profile with a conical shape, described by the equation [22]:

$$Q_r = \frac{2P}{\pi r_0^2 H}\left(1-\frac{z}{H}\right)\exp\left(1-\left(\frac{r}{r_0}\right)^2\right) \tag{1}$$

where Q_r is the input energy density (W/mm^3), P the absorbed laser beam power (W), and r_0, H, r and z are parameters that characterize the shape of the laser beam. The moving heat source was modeled by a user subroutine in SYSWELD.

During the LENS process, part of the energy generated by the laser beam is lost before being absorbed by the deposited material. Measurements done in Ref. [23] revealed that the laser energy transfer efficiency was in the range of 30 ~ 50%. This indicates that more than half of the incident laser energy is never transferred to the deposited material. There are many factors that can affect laser beam absorption. One of the main reasons is the laser beam irradiance on the fabricated part. Furthermore, other complex phenomena occur in the molten pool, such as solute partitioning, evaporation and marangoni convection, which are not taken into account in the current study. In this work, the nominal laser power is calibrated by matching the thermal profile surrounding the molten pool with the experimental data of Ref. [3]. The details and results of this calibration are reported in Ref. [18].

The model uses a fixed mesh for the plate and substrate, where the mesh elements of the plate are initially inactive and are activated during material deposition. Two different approaches are available to model material deposition in SYSWELD. One is activation/deactivation of elements,

which uses a formulation to activate and deactivate individual elements; another is the dummy material method. In the current study, a dummy material method that uses three different types of material is employed for the element activation. The first material is used for the substrate and the elements of layers that have already been deposited; this material is assigned the actual thermal and metallurgical properties of SS410. The initial phase of the substrate is assumed to be ferrite. Austenitization may occur when the temperature exceeds the austenitization temperature. The martensitic and ferritic transformations may occur during cooling in the substrate and in the layers that have been deposited, depending on the cooling rate and temperature. The second material is used for elements of layers that have not yet been deposited. These elements are assigned dummy low values of the thermal properties, which means that the material cannot be heated up, therefore cannot transform to austenite. No metallurgical properties (phase transformations) are required for the second material. A third type of material is used for the elements that are being deposited. These elements are initially in the dummy phase but they are assigned the actual thermal properties of SS410 so that they can heat up. Once they reach the austenization temperature, the dummy phase is switched to austenite and the actual metallurgical behavior (subsequent transformation to martensite or ferrite) is modeled after that. A graphical representation of the different material types is shown in Figure 2.

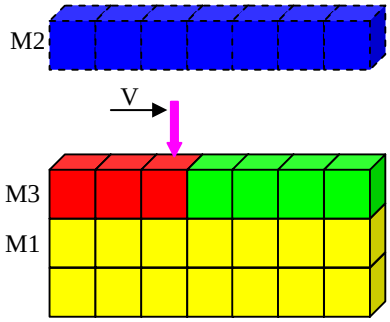

Figure 2. Sketch to illustrate the dummy material method for element activation. M1: deposited layers and substrate, material with actual thermal properties and phase transformation; M2: Layers to be deposited, material with dummy low thermal properties and no phase transformation; M3: Layer being deposited, material with actual thermal properties and dummy metallurgical phase.

Phase transformation model

Based on the thermal cycles at each point, the phase transformations that may occur in the material are predicted using semi-empirical models presented below.

Due to the high cooling rate surrounding the molten pool during the LENS process, diffusive solid-state transformations (e.g. ferritic-perlitic, and bainitic transformations) are usually suppressed during cooling to room temperature. As a result, the martensitic transformation occurs during the solidification. After the temperature drops below the martensite start temperature, M_s, the martensite transformation starts and the volume fraction of martensite increases as the material cools down. The volume fraction of martensite is given by the Koistinen-Marburger equation [19]:

$$p_m(T) = \bar{p}_m(1-\exp(-b(M_s - T))) \quad \text{for} \quad T \le M_s \tag{2}$$

where $\overline{p}_m$ represents the volume fraction of martensite obtained at an infinite low temperature ($\overline{p}_m$ is frequently assimilated to 1). The M_s temperature for SS410 is set at 350°C and b is the evolution coefficient of the transformation process, taken as 0.015 in this model [24]

The diffusive solid-state transformations may occur at locations far from the molten pool, such as the lower part of the plate close to the substrate, where lower cooling rate is obtained. For the phase transformations involving diffusion in steels (austenitic, ferritic-perlitic, and bainitic transformations), under isothermal conditions, the Johnson-Mehl-Avrami law is used [19]:

$$p(T,t) = \overline{p}(T)\left(1 - \exp\left(-\left(\frac{t}{\tau_R(T)}\right)^{n(T)}\right)\right) \tag{3}$$

where $\overline{p}$ represents the phase proportion obtained after an infinite time at temperature T, τ_R is the delay time, and n is the exponent associated with the reaction rate. The parameters of the Johnson-Mehl-Avrami model were extracted from the continuous cooling transformation (CCT) diagram according to the cooling rate and were inserted in the FE code in a tabular form.

Model Application

The model described in the previous section was calibrated with the experiments of Hofmeister *et al.* [3] in order to capture the effective laser power transferred to the material. The procedure, described in Ref. [18], showed a good agreement between the calculated results and experimental data for the temperature profile and cooling rate on the top surface of the part. In the present work, the thermally calibrated model was used to study the influence of the laser power and traverse speed on the final phase proportion and properties of a 10 layer thin-walled plate of AISI 410 stainless steel, deposited by the LENS process. The geometry used in the model is shown in Figure 3.

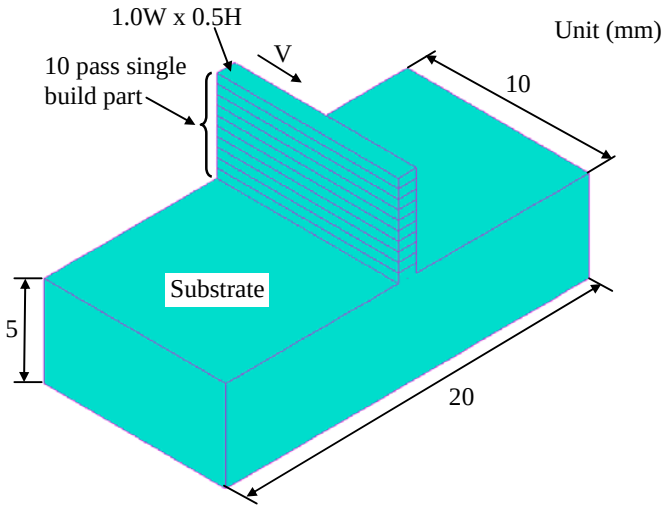

Figure 3. Geometry to simulate the LENS process for a 10 layer plate.

The structure was built by overlapping 10 single tracks of material, each with a length of 10.0 mm, a thickness of 0.5 mm and a width of 1.0 mm. The plate was fabricated on the surface of a

substrate having 5 mm thick, 10 mm wide and 20 mm long. Three cases are studied, when the traverse speed of the laser beam is 2.5 mm/s, 7.62 mm/s, and 20 mm/s. The idle time between depositions of consecutive layers for each case is 1.0s, 0.7s, and 0.5s, respectively. The laser beam moves in the same direction (left to right) for each pass.

Results and Discussions

The laser power is adjusted in order to achieve a steady molten pool size and temperature distribution surrounding the molten pool during the LENS process. Figure 4(a) shows the nominal laser power used for each pass at different traverse speeds. Higher laser power is required for higher traverse speed. A steady linear decrease of ~ 5% of the laser power is reached after deposition of the 5th layer. At the beginning of each pass, a higher laser power is applied in order to fully melt the powder, while a lower laser power is used near the end of each pass. The change of laser power for each pass is achieved by the laser power intensity, as shown in Figure 4 (b). The actual laser power is equal to the product of the nominal laser power and the laser power intensity.

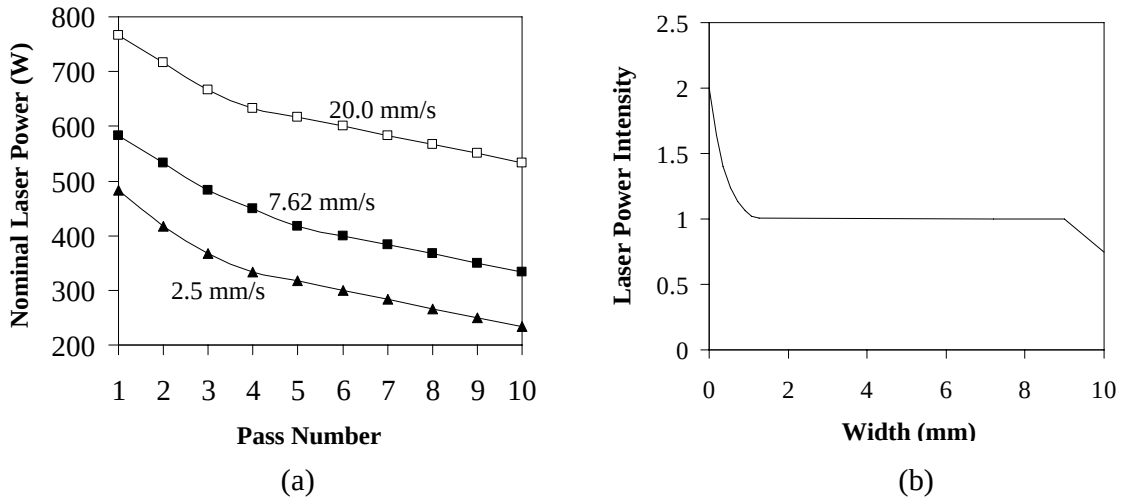

Figure 4. Laser power used in the study. (a) Nominal laser power distribution at each pass for different laser traverse speeds. (b) Laser power density along the travel direction from one side to another for each pass.

In order to achieve a fully dense material, previous layers should be melted as a new layer is deposited in order to maintain a continuous molten pool from layer to layer. The number of melted layers depends on the laser power and traverse speed chosen. Figure 5 shows the molten pool size and shape when the laser beam moves to the center of the part at the 10th layer for each laser traverse speed. The molten pool size is determined by the melting temperature of SS410 (1450°C). About one and a half layers are melted for each pass. It is observed that for the highest traverse speed (Figure 5(c)), the shape of the molten pool has become elongated and it hardly penetrates into the second layer.

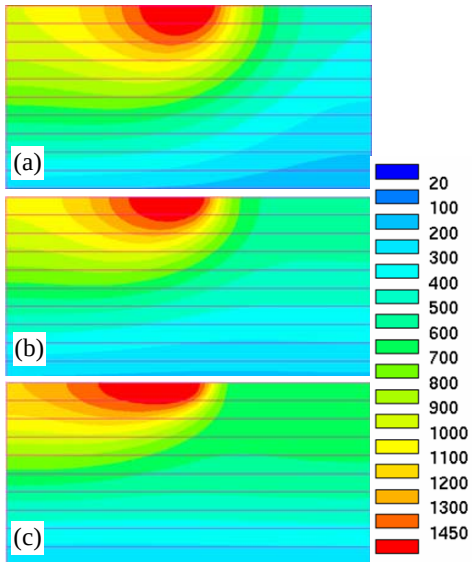

Figure 5. Molten pool size and shape when the laser beam moves to the center of the part at the 10th layer for different traverse speeds. The molten pool size is determined by the melting temperature of SS410 (1450°C). (a) V = 2.5 mm/s; b) V = 7.62 mm/s; c) V = 20 mm/s.

Figures 6, 7 and 8 show the temperature distribution and phase proportions for each traverse speed at the time instant after the 10th layer is deposited. Higher traverse speed keeps the upper region of the part at higher temperature (Figure 6(c)), which results in higher volume fraction of austenite (Figure 7(c)) and lower volume fraction of martensite (Figure 8(c)). The martensite present at lower layers is tempered martensite due to the thermal cycles. The austenite present at the upper layers will be transformed to fresh martensite and retained austenite when the part cools down to the room temperature. This will result in higher hardness at the upper layers than at the lower layers. These simulations clearly indicate that higher traverse speeds produce more volume fraction of austenite, which transform to fresh martensite, resulting in more uniform microstructure and higher hardness.

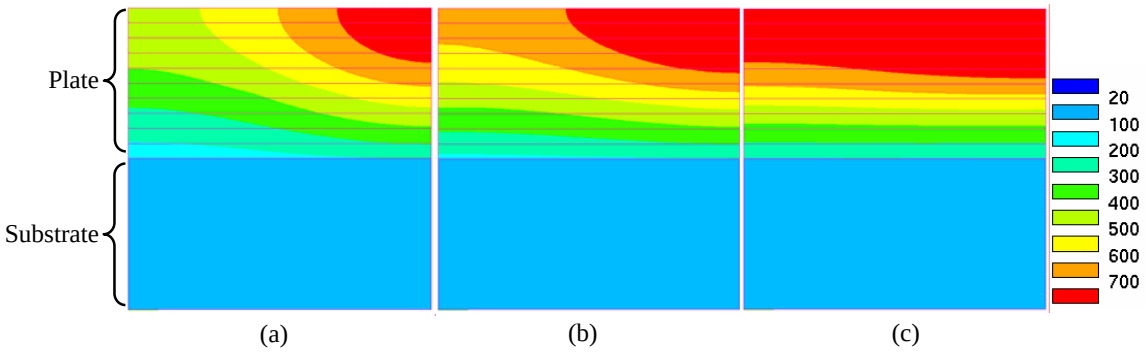

Figure 6. Temperature field at the time instant after the 10th layer is deposited. a) V = 2.5 mm/s; b) V = 7.62 mm/s; c) V = 20 mm/s.

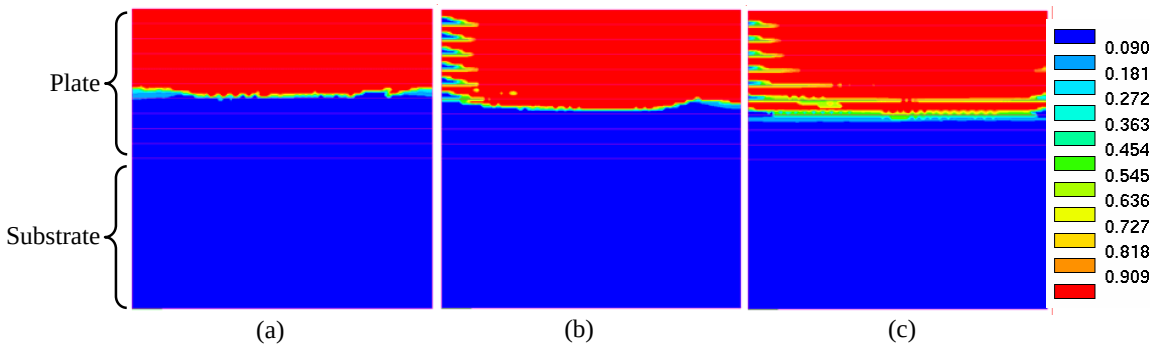

Figure 7. Volume fraction of austenite at the time instant after the 10th layer is deposited. a) V = 2.5 mm/s; b) V = 7.62 mm/s; c) V = 20 mm/s.

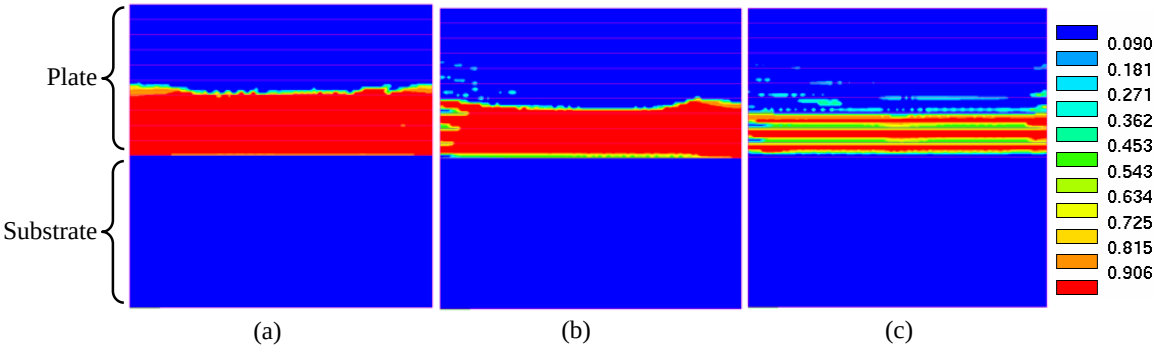

Figure 8. Volume fraction of martensite at the time instant after the 10th layer is deposited. a) V = 2.5 mm/s; b) V = 7.62 mm/s; c) V = 20 mm/s.

An undesired defect that may occur in LENS-deposited parts is the presence of porosity. The pores can result from gas evolution during solidification or lack of fusion between layers of consecutive depositions surrounding the molten pool [5]. In the current study, a low volume fraction of austenite is observed at the beginning of each layer, in particular for high traverse speed (Left side of Figure 7(b) and 7(c)). The blue stripes in these figures actually are unmelted elements that did not receive enough power for the current traverse speed. This occurs at the beginning of the layer deposition because this region has had more time to cool before the deposition of the next layer starts. Similarly, the low volume fraction of martensite present at the lower layers (Figure 8(c)) indicates the existence of unmelted powder due to the large heat dissipation of the substrate. Higher laser power is needed to fully melt the powder in the layers close to the substrate. These results provide some indications to illustrate the effect of the laser power and traverse speed on the porosity formation due to lack of fusion.

Conclusion

A three-dimensional finite element model has been developed and implemented to simulate the LENS deposition of a SS410 plate. The model was used to analyze the temperature distribution, molten pool size, and volume fraction of the solid phases formed at different traverse speeds. The laser power should be adjusted for each pass during the LENS deposition in order to keep a steady molten pool size. The modeling results show that a higher traverse speed can reduce the proportion of tempered martensite and achieve more uniform microstructure and hardness

distribution in the plate. This is because a higher traverse speed allows most of the part to remain at temperatures higher than the martensite start temperature through the process, before it cools down to room temperature after the deposition is finished. However, higher traverse speeds can lead to the presence of porosity due to lack of fusion, particularly in the layers close to the substrate. Enough laser power is required for high traverse speeds in order to completely melt the powder and obtain a dense material.

Acknowledgements

The authors appreciate the sponsorship of the U.S. Army TACOM and the Center for Advanced Vehicular Systems (CAVS). We would like to thank Dr. John Berry of Mississippi State University, Jim Bullen of Optomec Co. and Benton Gady of National Automotive Center (NAC) for their helpful suggestions and guidance in this work. The support of Dr. Yogendra Gooroochurn (ESI) with SYSWELD is also appreciated.

References

1. M.L. Griffith et al., "Understanding the Microstructure and Properties of Components Fabricated by Laser Engineered Net Shaping (LENS)," *Materials Research Society*, Symposium Y Proceedings, 625 (2000), 9-20.

2. M.L. Griffith et al., "Understanding Thermal Behavior in the LENS Process," *Journal of Materials Design*, 20 (1999), 107-114.

3. W. Hofmeister et al., "Investigation of Solidification in the Laser Engineered Net Shaping (LENS) Process," JOM 51 (1999), available from JOM-*e* online at www.tms.org/pubs/journals/JOM/9907/Hofmeister/Hofmeister-9907.html.

4. C.L. Atwood et al., "Laser Engineered Net Shaping (LENS): A Tool for Direct Fabrication of Metal Parts," Proceedings of ICALEO '98, Orlando, FL, November 16-19, 1998, E-1-E-7.

5. G.K. Lewis, and E. Schlienger, "Practical Considerations and Capabilities for Laser Assisted Direct Metal Deposition," *Materials and Design*, 21 (2000), 417-423.

6. M.L. Griffith et al., "Thermal Behavior in the LENS^{TM} Process," Proceedings of the Solid Freeform Fabrication Symposium, Austin, TX, 1998, 89-97.

7. R. Ye et al., "Numerical Modeling of the Thermal Behavior during the LENS process," *Materials Science and Engineering A*, 428 (2006), 47-53.

8. L. Wang and S. Felicelli, "Analysis of Thermal Phenomena in LENS^{TM} Deposition," *Materials Science and Engineering A*, 435-436 (2006), 625-631.

9. R. Colaco, and R. Vilar, "Stabilization of Retained Austenite in Laser Surface melted Tool Steels," *Materials Science and Engineering A*, 385 (2004), 123-127.

10. R. Colaco and R. Vitar, "Effect of Laser Surface Melting on the Tempering Behavior of DIN X42Cr13 Stainless Tool Steel," *Scripta Materialia*, 38 (1998), 107-113.

11. R. Colaco and R. Vitar, “Effect of the Processing Parameters on the Proportion of Retained Austenite in Laser Surface Melted Tool Steels,” *Journal of Materials Science Letters*, 17 (1998), 563-567.

12. Costa et al., “Rapid Tooling by Laser Powder Deposition: Process Simulation Using Finite Element Analysis,” *Acta Materialia*, 53 (2005), 3987-3999.

13. L. Costa et al., “Simulation of Layer Overlap Tempering Kinetics in Steel Parts Deposited by Laser Cladding,” In: Keicher D., Sears J.W., Smugeresky J.E., editors. Proceedings of International Conference on Metal Powder Deposition for Rapid Manufacturing. Princeton (NJ): MPIF; 2002, 172-176.

14. L. Costa et al., “Simulation of Phase Transformations in Steel Parts Produced by Laser Powder Deposition,” *Materials Science Forum*, 473-474 (2005), 315-320.

15. S.M. Kelly, and S.L. Kampe, “Microstructural evolution in laser-deposited multilayer Ti-6Al-4V builds: Part II. Thermal Modeling,” *Metallurgical and Materials Transactions A*, 35 (2004), 1869-1879.

16. M. Labudovic, D. Hu, and R. Kovacevic, “A Three Dimensional Model for Direct Laser Metal Powder Deposition and Rapid Prototyping,” *Journal of Materials Science*, 38 (2003), 35-49.

17. A. Vasinonta, J.L. Beuth, and M.L. Griffith, “Process Maps for Controlling Residual Stress and Melt Pool Size in Laser-based SFF Processes,” Proceedings of the Solid Freeform Fabrication Symposium, Austin, TX, August, 2000.

18. L. Wang et al., “Numerical Simulation of the Temperature Distribution and Solid-phase Evolution in the LENS^{TM} Process,” Proceedings of the Seventeenth Solid Freeform Fabrication Symposium, Austin, TX, August, 2006.

19. SYSWELD 2005 Reference Manual, ESI Group, 2005.

20. SYSWELD 2005 Example Manual, ESI Group, 2005.

21. SYSTUS 2005 Analysis Reference Manual, ESI Group, 2005.

22. S.A. Tsirkas, P. Papanikos, and Th. Kermanidis, “Numerical Simulation of the Laser Welding Process in Butt-joint Specimens,” *Journal of Materials Processing Technology*, 134 (2003), 59-69.

23. R.R. Unocic, and J.N. DuPont, “Process Efficiency Measurements in the Laser Engineered Net Shaping Process,” *Metallurgical and Materials Transactions B*, 35 (2004), 143-152.

24. ASM Handbook, Welding, Brazing, and Soldering, Vol. 6, ASM International, Material Park, OH, 2005, 438.